AIP Advances

Control of optical bistability and third-order nonlinearity via tunneling induced quantum interference in triangular quantum dot molecules

Si-Cong Tian, Ren-Gang Wan, Cun-Zhu Tong, Jin-Long Zhang, Xiao-Nan Shan, Xi-Hong Fu, Yu-Gang Zeng, Li Qin, and Yong-Qiang Ning

Citation: AIP Advances **5**, 067144 (2015); doi: 10.1063/1.4922959
View online: http://dx.doi.org/10.1063/1.4922959
View Table of Contents: http://scitation.aip.org/content/aip/journal/adva/5/6?ver=pdfcov
Published by the AIP Publishing

Control of optical bistability and third-order nonlinearity via tunneling induced quantum interference in triangular quantum dot molecules

Si-Cong Tian,[1,a] Ren-Gang Wan,[2] Cun-Zhu Tong,[1,b] Jin-Long Zhang,[1] Xiao-Nan Shan,[1] Xi-Hong Fu,[1] Yu-Gang Zeng,[1] Li Qin,[1] and Yong-Qiang Ning[1]

[1]*State Key laboratory of Luminescence and Applications, Changchun Institute of Optics, Fine Mechanics and Physics, Chinese Academy of Sciences, Changchun 130033, China*

[2]*School of Physics and Information Technology, Shaanxi Normal University, Xi'an 710062, China*

(Received 15 April 2015; accepted 9 June 2015; published online 22 June 2015)

The optical bistability of a triangular quantum dot molecules embedded inside a unidirectional ring cavity is studied. The type, the threshold and the hysteresis loop of the optical bistability curves can be modified by the tunneling parameters, as well as the probe laser field. The linear and nonlinear susceptibilities of the medium are also studied to interpret the corresponding results. The physical interpretation is that the tunneling can induce the quantum interference, which modifies the linear and the nonlinear response of the medium. As a consequence, the characteristics of the optical bistability are changed. The scheme proposed here can be utilized for optimizing and controlling the optical switching process. [http://dx.doi.org/10.1063/1.4922959]

I. INTRODUCTION

Optical bistability (OB), which has been extensively investigated in the recent past years, has potential application in the field of optical logic, all optical switching, and optical transistors. Most of the theoretical and experimental studies in OB have been committed to two-level atomic systems in optical resonators.[1–7] In these systems, the cavity field intensity can only be controlled by its own input field. Therefore, how to control OB artificially has attracted a lot of interest in this research region. In three-level[8–14] or four-level[15–18] atomic systems, the coupling fields can induce quantum interference, which can greatly modify the OB behavior of the system.

On the other hand, quantum dots (QDs) has many advantages over atoms, and that is, large electric-dipole moments, high nonlinear optical coefficients, customized design and ease of integration. When two or more QDs are placed closely, quantum dot molecules (QDMs) can be built. By using self assembled dot growth technology, double quantum dots (DQDs) can be fabricated experimentally.[19] With the help of an external electric field,[20–22] the tunneling between the dots can induce quantum interference and coherence.[23–25] Therefore, fundamental studies such as electromagnetically induced transparency (EIT),[26,27] coherent population transfer,[28–31] optical bistability,[32–35] entanglement,[36,37] narrowing of fluorescence spectrum[38] and enhanced self-Kerr nonlinearity[39] are studied. Furthermore, triple quantum dots (TQDs) are receiving much attention, due to its multilevel structure and extra controlling parameters which can not be found in DQDs. TQDs composed of linear or triangular type have been fabricated in much experimental progress.[40–43] Theoretical works of TQDs such as transmission-dispersion spectrum,[44] multiple transparency windows and cavity linewidth narrowing,[45,46] Kerr nonlinearity[47] and resonance fluorescence spectrum[48] are studied.

[a]Electronic mail: tiansicong@ciomp.ac.cn
[b]Electronic mail: tongcz@ciomp.ac.cn

In this paper, we investigate the OB characters of the triangular TQDs embedded in a unidirectional ring cavity. The two tunneling couplings can induce quantum interference and modify the nonlinearity of the medium, leading to the changing of the OB behavior. Our work is based primarily on the previous studies. The Differences between ours and previous ones are mainly in the following three points. First, in multi-level atomic systems OB is modified by coupling lasers.[8–18] But here we use tunneling coupling to induce quantum interference and modify the OB properties. Second, the using of two tunneling couplings in TQDs brings flexibility to the control of OB, which can not be achieved in DQDs.[32–35] Third, though OB has been recently studied in TQDs,[49,50] our study is different from those in the following ways: the incoherent pump is not included; the effect of the third-order nonlinearity is taken into.

II. MODEL AND EQUATIONS

The setup of the triangular TQDs is shown in Fig. 1(a). Three QDs are arranged triangularly, and both QD 2 and QD 3 are coupled to QD 1 with two gate electrodes, which can be used to control the tunneling between the neighbor dots. Fig. 1(b) shows the energy level of the triangular TQDs. The system consists of four levels, which are ground state $|0\rangle$, direct exciton state $|1\rangle$ and two indirect exciton states $|2\rangle$ and $|3\rangle$, as described before.[45,46] Compared with linear TQDs, the main difference is that in triangular type, states $|2\rangle$ and $|3\rangle$ are both coupled to state $|1\rangle$ individually.

The Hamiltonian of the basis $\{|0\rangle, |1\rangle, |2\rangle, |3\rangle\}$ under the rotating-wave and the electric-dipole approximations can be written as (assumption of $\hbar = 1$)

$$H_I = \begin{pmatrix} 0 & -\Omega_p & 0 & 0 \\ -\Omega_p & \delta_p & -T_2 & -T_3 \\ 0 & -T_2 & \delta_p - \omega_{12} & 0 \\ 0 & -T_3 & 0 & \delta_p - \omega_{13} \end{pmatrix}. \tag{1}$$

Here $\Omega_p = \mu_{01} E_p$ denotes the Rabi frequency of the laser field, with E_p being the electric field amplitude, and $\mu_{01} = \boldsymbol{\mu}_{01} \cdot \mathbf{e}$ being the electric dipole moment of transition $|0\rangle \leftrightarrow |1\rangle$. ($\mathbf{e}$ is the polarization vector.) T_2 and T_3 are the coupling intensity of the two tunnelings, and they relay on the intrinsic sample barrier, as well as the extrinsic electric field. The detuning of the laser field is defined as $\delta_p = \omega_{10} - \omega_p$, where ω_p is the laser frequency, and ω_{10} is the transition frequency of the exited state $|1\rangle$ and ground state $|0\rangle$. ω_{12} and ω_{13} are the energy splittings of the excited states, and they relay on the effective confinement potential manipulated by the external voltage.

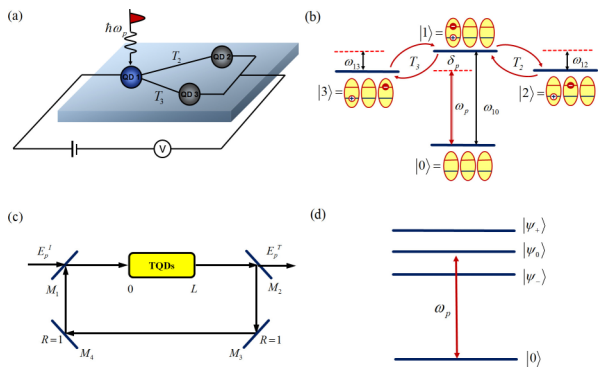

FIG. 1. (a) The schematic of the setup of the triangular TQDs. The probe field transmits the QD 1. The wavelengths of the probe field depends on the sample structure, and it could be around 870nm according to Ref. 22. V is a bias voltage, which is supposed to be several hundreds Millivolt.[19,25] (b) The schematic of the level configuration of the triangular TQDs. (c) Unidirectional ring cavity containing a triangular TQDs sample of length L, $E_p{}^I$ and $E_p{}^T$ are the incident and the transmitted field, respectively. And this type of cavity with atomic sample has already been achieved in experiments.[14,15,18] (d) Dressed states of the triangular TQDs for two tunneling couplings.

The state vector at time t is

$$|\Psi_I(t)\rangle = a_0(t)|0\rangle + a_1(t)|1\rangle + a_2(t)|2\rangle + a_3(t)|3\rangle, \tag{2}$$

which obeys the Schrödinger equation

$$\frac{d}{dt}|\Psi_I(t)\rangle = -iH_I(t)|\Psi_I(t)\rangle. \tag{3}$$

Substituting Eq. (1) and (2) into Eq. (3), and using the Weisskopf-Wigner theory,[51,52] the dynamical equations for the atomic probability amplitudes in the interaction picture can be obtained:

$$i\dot{a}_0 = -\Omega_p a_1, \tag{4a}$$

$$i\dot{a}_1 = -\Omega_p a_0 - T_2 a_2 - T_3 a_3 + \left(\delta_p - i\gamma_1\right) a_1, \tag{4b}$$

$$i\dot{a}_2 = -T_2 a_1 + \left(\delta_p - \omega_{12} - i\gamma_2\right) a_2, \tag{4c}$$

$$i\dot{a}_3 = -T_3 a_1 + \left(\delta_p - \omega_{13} - i\gamma_3\right) a_3, \tag{4d}$$

with $|a_0|^2 + |a_1|^2 + |a_2|^2 + |a_3|^2 = 1$. And here $\gamma_i = \frac{1}{2}\Gamma_{i0} + \gamma_{i0}^d (i = 1 - 3)$ are typical effective decay rates, which are contributed by two parts, radiative decay rate Γ_{i0} from $|i\rangle \rightarrow |0\rangle$ and the pure dephasing rate γ_{i0}^d.

Then we consider the TQDs embedded in the cavity [Fig. 1(c)]. The cavity comprises four mirrors. And the intensity reflection coefficient of mirrors 1 and the intensity transmission coefficient of mirrors 2 are R and T, respectively, and they satisfy the condition of $R + T = 1$. The mirrors 3 and 4 are assumed to have 100% reflectivity. The probe laser field circulates through the ring cavity and its electromagnetic field is $E = E_p e^{-i\omega_p t}$ + c.c. ("c.c." means the complex conjugation). When the probe field goes through TQDs medium, because of the induced polarization in the intersubband transitions $|0\rangle \rightarrow |1\rangle$, the absorption and dispersion properties of the probe field will be modified. And the slowly oscillating term of the induced polarization $P(\omega_p)$ is determined by

$$P(\omega_p) = \frac{\Gamma}{V}\mu_{01}\rho_{10}. \tag{5}$$

Here $\rho_{10} = a_0 a_1^*$ is the density matrix element, Γ is the optical confinement factor, and V is the volume of the TQDs.[20,21]

Then the dynamic response of the probe laser field under the slowly varying envelope approximation, can be governed by Maxwell's equation,

$$\frac{\partial E_p}{\partial t} + c\frac{\partial E_p}{\partial z} = i\frac{\omega_p}{2\varepsilon_0}P(\omega_p), \tag{6}$$

where c is the light speed and ε_0 is the permittivity of the free space. In the steady-state case, the time derivative in Eq. (6) is set to zero, then the field amplitude can be written as

$$\frac{\partial E_p}{\partial z} = i\frac{\Gamma}{V}\frac{\omega_p\mu_{01}}{2c\varepsilon_0}\rho_{10}. \tag{7}$$

In our case, the boundary conditions is

$$E_p(0) = \sqrt{T}{E_p}^I + RE_p(L), \tag{8a}$$

$$E_p(L) = {E_p}^T/\sqrt{T}, \tag{8b}$$

where ${E_p}^I$ is the incident field, ${E_p}^T$ is the transmitted field and L is the sample length. And $RE_p(L)$ in Eq. (8a) presents the feedback mechanism by mirrors.

In the mean-field limit,[53,54] by using Eq. (8) the input-output equation is

$$y = x - iC\rho_{10}, \tag{9a}$$

$$y = \mu_{01}{E_p}^I/\hbar\sqrt{T}, \tag{9b}$$

$$x = \mu_{01}{E_p}^T/\hbar\sqrt{T}. \tag{9c}$$

Here $C = \frac{\Gamma}{V}\frac{\omega_p L|\mu_{01}|^2}{2\hbar c\varepsilon_0 T}$ is the electronic cooperation parameter. It is worthwhile stressing that $iC\rho_{10}$ in Eq. (9a) is essential for the occurring of the OB. Solve Eq. (4) by the method used in Ref. 47 (see the Appendix), then the expression of ρ_{10} is

$$\rho_{10} = \frac{\Omega_p}{\Gamma_1 - \frac{T_2^2}{\Gamma_2} - \frac{T_3^2}{\Gamma_3}} \frac{1}{1 + \frac{{\Omega_p}^2}{\left|\Gamma_1 - \frac{T_2^2}{\Gamma_2} - \frac{T_3^2}{\Gamma_3}\right|^2}\left(1 + \frac{T_2^2}{|\Gamma_2|^2} + \frac{T_3^2}{|\Gamma_3|^2}\right)}, \tag{10}$$

where $\Gamma_1 = \delta_p - i\gamma_1$, $\Gamma_2 = \delta_p - \omega_{12} - i\gamma_2$, $\Gamma_3 = \delta_p - \omega_{13} - i\gamma_3$. Then together with Eq. (9a), we can reach the intensity of the output field versus the intensity of the input field in the steady state solutions.

Since the OB behavior is the results of nonlinearity of the interaction of the atomic medium and feedback of the optical intercavity field, the nonlinear susceptibility of the system is necessary. It is well known that the polarization of the medium can also be written as

$$P(\omega_p) = \varepsilon_0 \chi_p E_p. \tag{11}$$

Together with Eq. (6), the probe susceptibility can be obtained,

$$\chi_p = \frac{\Gamma}{V}\frac{{\mu_{01}}^2}{\varepsilon_0\hbar}\frac{\rho_{10}}{\Omega_p} = \frac{\Gamma}{V}\frac{{\mu_{01}}^2}{\varepsilon_0\hbar}\chi. \tag{12}$$

Here $\chi = \rho_{10}/\Omega_p$ is independent of the product of Γ/V. Using the Maclaurin formula and neglecting the higher-order smaller terms,[47] χ can be expanded into the second order of Ω_p,

$$\chi = \chi^{(1)} + \chi^{(3)}{\Omega_p}^2, \tag{13}$$

where $\chi^{(1)}$ and $\chi^{(3)}$ correspond to the first-order linear and third-order nonlinear parts of the susceptibility, respectively, and they are given by

$$\chi^{(1)} = \frac{1}{\Gamma_1 - \frac{T_2^2}{\Gamma_2} - \frac{T_3^2}{\Gamma_3}}, \tag{14a}$$

$$\chi^{(3)} = -\frac{1}{\Gamma_1 - \frac{T_2^2}{\Gamma_2} - \frac{T_3^2}{\Gamma_3}} \frac{1}{\left|\Gamma_1 - \frac{T_2^2}{\Gamma_2} - \frac{T_3^2}{\Gamma_3}\right|^2}\left(1 + \frac{T_2^2}{|\Gamma_2|^2} + \frac{T_3^2}{|\Gamma_3|^2}\right). \tag{14b}$$

In the next part, according to Eq. (9a) we show some results of OB under various parametric conditions. And also the linear and nonlinear susceptibilities are calculated to interpret these OB characters. In our calculations, the value of the parameters are based on Ref. 47 and references therein, and the values are realistic and scaled by γ_1.

III. RESULTS AND DISCUSSIONS

First we consider the case of $\omega_{12} = \omega_{13}$ and show in Fig. 2(a) the OB behavior for $\delta_p = 0$ under the different tunneling coupling situation. When no tunneling is applied, the electron will be trapped in QD 1. Thus we can obtain a OB of the two-level single QD system [red solid line]. Then when tunneling T_2 is applied, the system turns to be the three-level DQDs for electrons can tunnel from QD 1 to QD 2. In this case, the OB disappears (the situation for applying tunneling T_3 is the same) [blue dashed line]. With both tunneling T_2 and T_3, the electrons will tunnel from QD 1 to QD 2 or QD 3. Thus the system goes to four-level TQDs, but still the OB does not appear [blue dashed line].

To interpret the above results, we show in Fig. 2(b)-2(d) the linear absorption Im$[\chi^{(1)}]$, nonlinear absorption Im$[\chi^{(3)}]$ and nonlinear dispersion Re$[\chi^{(3)}]$ versus the frequency detuning of the probe field δ_p, respectively. As can be seen, without tunneling, Im$[\chi^{(1)}]$ and Im$[\chi^{(3)}]$ both have nonzero value for $\delta_p = 0$, which is responsible for the appearance of OB. Besides the nonlinear dispersion for $\delta_p = 0$ is zero, therefore the type of OB is absorptive. On the contrary, with one or two tunneling, the linear, nonlinear absorption and nonlinear dispersion are all reduced to zero for $\delta_p = 0$, resulting in the disappearance of OB.

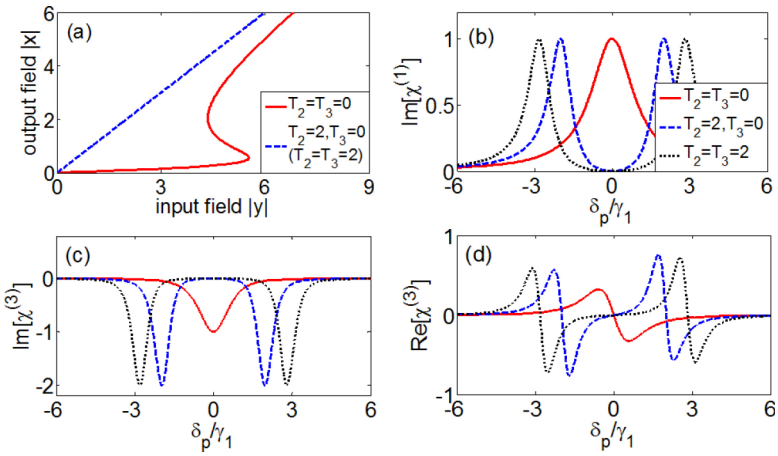

FIG. 2. (a) Output intensity $|x|$ versus input intensity $|y|$ for $\delta_p = 0$, (b) imaginary $\mathrm{Im}[\chi^{(1)}]$ parts of the linear susceptibility, (c) imaginary $\mathrm{Im}[\chi^{(3)}]$ and (d) real $\mathrm{Re}[\chi^{(3)}]$ parts of the nonlinear susceptibility as a function of probe detuning δ_p, respectively. Other parameters are $\omega_{12} = \omega_{13} = 0$, $\gamma_2 = \gamma_3 = 10^{-3}\gamma_1$, and $C = 20$. (All parameters are scaled by the decay rate γ_1).

To see the physical interpretation clearly the dressed state should be used. To do that, the Hamiltonian corresponding to the system and the tunneling coupling needs to be diagonalized. Then the expressions of the dressed states [Fig. 1(d)] to the first order in T_3 are

$$|\psi_+\rangle = \frac{1}{D_+}\left[(\Omega_R + \omega_{12}/2)\,|1\rangle - T_2\,|2\rangle - \frac{T_3\,(\Omega_R + \omega_{12}/2)}{(\Omega_R + \omega_{13} - \omega_{12}/2)}\,|3\rangle\right], \tag{15a}$$

$$|\psi_-\rangle = \frac{1}{D_-}\left[(\Omega_R - \omega_{12}/2)\,|1\rangle + T_2\,|2\rangle - \frac{T_3\,(\Omega_R - \omega_{13}/2)}{(\Omega_R - \omega_{13} + \omega_{12}/2)}\,|3\rangle\right], \tag{15b}$$

$$|\psi_0\rangle = |\omega_{12} - \omega_{13}|\left[\frac{T_3}{{D_0}^2}\,|1\rangle - \frac{T_2 T_3}{(\omega_{12} - \omega_{13})\,{D_0}^2}\,|2\rangle + \frac{1}{(\omega_{12} - \omega_{13})}\,|3\rangle\right], \tag{15c}$$

where

$$D_+ = \sqrt{(\omega_{12}/2 + \Omega_R)^2 + {T_2}^2}, \tag{16a}$$

$$D_- = \sqrt{(\omega_{12}/2 - \Omega_R)^2 + {T_2}^2}, \tag{16b}$$

$${D_0}^2 = \left|\omega_{13}\,(\omega_{12} - \omega_{13}) + {\Omega_R}^2\right|, \tag{16c}$$

with $\Omega_R \equiv \sqrt{(\omega_{12}/2)^2 + {T_2}^2}$. And the eigenvalues are $E_+ = \delta_p - \omega_{12}/2 + \Omega_R$, $E_- = \delta_p - \omega_{12}/2 - \Omega_R$ and $E_0 = \delta_p - \omega_{13}$.

From Eq. (15), in the case of $T_3 \to 0$ (similar to DQDs), the dressed state $|\Psi_0\rangle$ coincides with the bare state $|3\rangle$, so it is decoupled from the system. The other two dressed states $|\Psi_\pm\rangle$ are Autler-Townes components, and the energy splitting of them is Ω_R. For $|\Psi_\pm\rangle$ have a finite overlap with the excited state $|1\rangle$, there exists quantum interference in two transitions $|0\rangle \to |\Psi_\pm\rangle$. And the quantum interference suppresses both $\mathrm{Im}[\chi^{(1)}]$ and $\mathrm{Im}[\chi^{(3)}]$, leading to the disappearance of the OB. If $T_3 \neq 0$, $\omega_{12} = \omega_{13}$ will also lead dressed level $|\Psi_0\rangle$ to decouple from the system, and still the OB does not show up. So in the following we will only investigate the OB behavior of TQDs for $\omega_{12} \neq \omega_{13}$. In this case, all dressed states $|\Psi_i\rangle\,(i = 0, +, -)$ contain an admixture of $|1\rangle$, so quantum interference arises in all transitions $|0\rangle \to |\Psi_i\rangle\,(i = 0, +, -)$, and modifies the linear and nonlinear susceptibilities of the TQDs, resulting in the appearance of the OB.

In Figs. 3–5, we investigate the OB behavior of TQDs considering $\omega_{12} \neq \omega_{13}$. And for simplicity, we only consider the case of $\omega_{12} = -\omega_{13} = \omega$ and $T_2 = T_3 = T$. First we show in Fig. 3(a) the OB curves for $\delta_p = 0$ under the different tunneling T. As the tunneling T is increasing, the threshold of OB is decreased, while the slope of lower branch of OB keeps the same. To interpret these results we

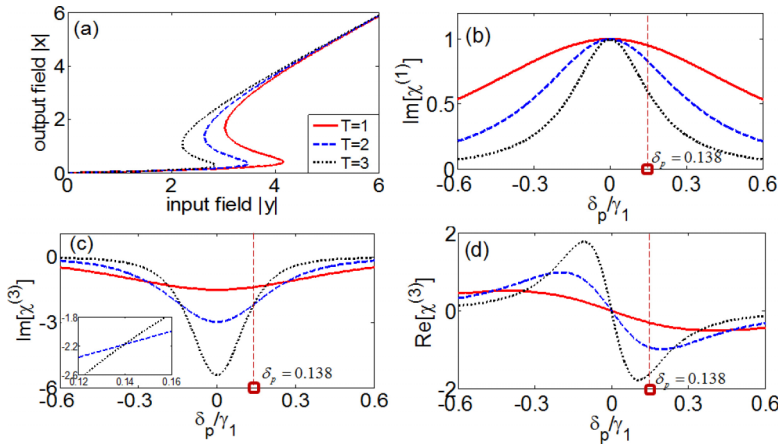

FIG. 3. (a) Output intensity $|x|$ versus input intensity $|y|$ for $\delta_p = 0$, (b) imaginary $\mathrm{Im}[\chi^{(1)}]$ parts of the linear susceptibility, (c) imaginary $\mathrm{Im}[\chi^{(3)}]$ and (d) real $\mathrm{Re}[\chi^{(3)}]$ parts of the nonlinear susceptibility as a function of probe detuning δ_p, respectively. Other parameters are the same as those in Fig. 2, except that $\omega_{12} = -\omega_{13} = \omega = 2$.

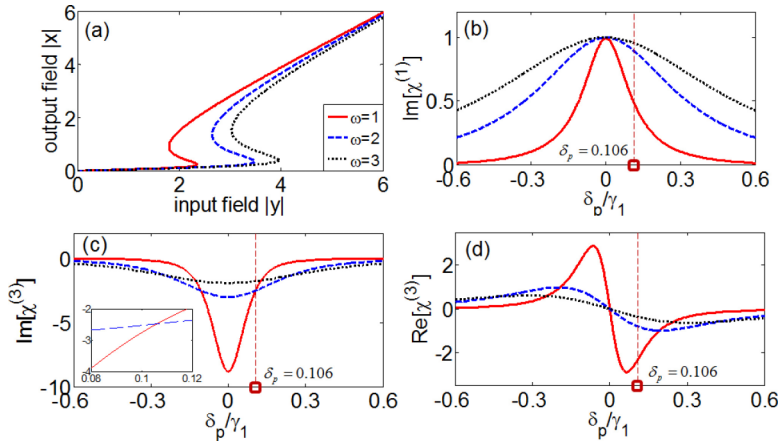

FIG. 4. (a) Output intensity $|x|$ versus input intensity $|y|$ for $\delta_p = 0$, (b) imaginary $\mathrm{Im}[\chi^{(1)}]$ parts of the linear susceptibility, (c) imaginary $\mathrm{Im}[\chi^{(3)}]$ and (d) real $\mathrm{Re}[\chi^{(3)}]$ parts of the nonlinear susceptibility as a function of probe detuning δ_p, respectively. Other parameters are the same as those in Fig. 2, except that $T_2 = T_3 = T = 2$.

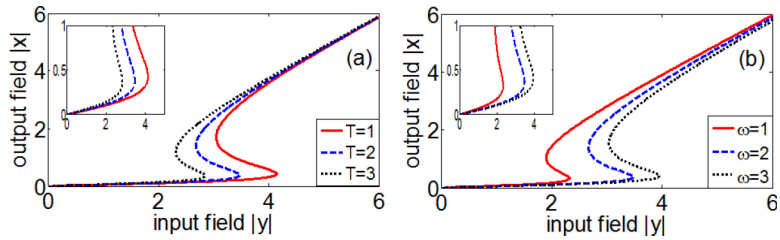

FIG. 5. (a) Output intensity $|x|$ versus input intensity $|y|$ for different value of T. Parameters are $\delta_p = 0.138$ and $\omega = 2$. (b) Output intensity $|x|$ versus input intensity $|y|$ for different value of ω. Parameters are $\delta_p = 0.106$ and $T = 2$. Other parameters are the same as those in Fig. 2.

show in Fig. 3(b)–3(d) the linear absorption $\mathrm{Im}[\chi^{(1)}]$, nonlinear absorption $\mathrm{Im}[\chi^{(3)}]$ and nonlinear dispersion $\mathrm{Re}[\chi^{(3)}]$, respectively. When $\delta_p = 0$, both $\mathrm{Im}[\chi^{(1)}]$ and $\mathrm{Im}[\chi^{(3)}]$ have a nonzero value, while $\mathrm{Re}[\chi^{(3)}]$ keeps zero. Therefore the type of OB is absorptive for all three cases. And with the increasing value of T, $\mathrm{Im}[\chi^{(1)}]$ keeps unchanged [Fig. 3(b)], while $\mathrm{Im}[\chi^{(3)}]$ is increased [Fig. 3(c)]. Therefore it can be deduced that the linear absorption is in charge of the slope of lower branch of the absorptive OB, and the nonlinear absorption is in charge of the threshold of the absorptive OB.

Next we show the effects of the energy splitting ω on the OB for $\delta_p = 0$ in Fig. 4(a). As can be seen that the increasing of ω leads to the increased threshold of OB, but the slope of lower branch of OB does not change. The behavior of OB can also be interpreted by the linear and nonlinear susceptibilities. As can be seen from Fig. 4(b), for certain detuning $\delta_p = 0$, with increasing value of ω the value of $\mathrm{Im}[\chi^{(1)}]$ for $\delta_p = 0$ is the same, resulting in the same slope of lower branch of OB. While $\mathrm{Im}[\chi^{(3)}]$ is reduced [Fig. 4(c)], which leads to the increased threshold of OB. And for all values of ω, the nonlinear dispersion $\mathrm{Re}[\chi^{(3)}]$ is zero [Fig. 4(d)], therefore the type of the OB is also absorptive.

From the above discussion of Fig. 3 and 4, one can conclude that the OB behavior can be controlled by the tunneling intensity or the energy splitting. The physical explanation is that the increasing value of T or the decreasing value of ω can lead to the increased nonlinear absorption, which makes the cavity field easier to reach saturation, so the threshold of OB is decreased.

The above results are obtained for $\delta_p = 0$. For further investigations, we show in Fig. 5 the OB curves for $\delta_p \neq 0$. First we choose typical detuning $\delta_p = 0.138$ and plot in Fig. 5(a) the OB curves for various values of tunneling T. As T is increasing, the threshold of OB is decreased, while the slope of lower branch of OB is increased. These results can be understood by Fig. 3(b)-3(d). For all cases, $\mathrm{Im}[\chi^{(1)}]$, $\mathrm{Im}[\chi^{(3)}]$ and $\mathrm{Re}[\chi^{(3)}]$ are not zero, therefore the OB is hybrid absorptive-dispersive type. And with the increasing value of T, $\mathrm{Im}[\chi^{(1)}]$ is decreased [Fig. 3(b)], as a result, the slope of lower branch of OB is increased. And from Fig. 3(c), $\mathrm{Im}[\chi^{(3)}]$ for $T = 1$ is smaller than that of for $T = 2$ and $T = 3$, as a result, the threshold of OB for $T = 1$ is larger than the other two cases. Furthermore, $\mathrm{Re}[\chi^{(3)}]$ is increased as T is increasing [Fig. 3(d)]. Although $\mathrm{Im}[\chi^{(3)}]$ for $T = 2$ and for $T = 3$ is the same [inset of Fig. 3(c)], the larger value of $\mathrm{Re}[\chi^{(3)}]$ also leads to the smaller threshold of OB. Thus one can deduce that the nonlinear dispersion can modify the threshold of OB as well. The larger value of nonlinear dispersion will lead to the smaller threshold of OB.

Next we choose $\delta_p = 0.106$ and show in Fig. 5(b) the influence of energy splitting ω on the OB behavior. From the figure one can see that the increasing of ω leads to the increased threshold of OB and the decreased slope of lower branch of OB. These results can be understood by Fig. 4(b)-4(d). Because of the nonzero value of $\mathrm{Im}[\chi^{(1)}]$, $\mathrm{Im}[\chi^{(3)}]$ and $\mathrm{Re}[\chi^{(3)}]$, the OB is also hybrid absorptive-dispersive type for all three cases. And $\mathrm{Im}[\chi^{(1)}]$ is increased as ω is increasing [Fig. 4(b)], resulting in the decreased slope of lower branch of OB. From Fig. 4(c), $\mathrm{Im}[\chi^{(3)}]$ for $\omega = 3$ is smaller than that of for $\omega = 1$ and $\omega = 2$, thererfore the threshold of OB for $\omega = 3$ is larger than the other two cases. And with increasing of ω the value of $\mathrm{Re}[\chi^{(3)}]$ is decreased [Fig. 4(d)]. Although $\mathrm{Im}[\chi^{(3)}]$ for $\omega = 1$ and for $\omega = 2$ is the same [inset of Fig. 4(c)], the larger value of $\mathrm{Re}[\chi^{(3)}]$ also results in the smaller threshold of OB. So once again, the nonlinear dispersion is in charge of the changing of the threshold of OB.

Last we show in Fig. 6 the impact of the types of OB on the hysteresis loop. In Fig. 6(a), the OB curves are obtained under the same parameters used in Fig. 3(a) except for $\delta_p = 0.25$. From the dotted line ($T = 3$) in Fig. 3(c) and 3(d), for $\delta_p = 0.25$ the value of $\mathrm{Im}[\chi^{(3)}]$ is nearly zero, while the value of $\mathrm{Re}[\chi^{(3)}]$ is nonzero, therefore, the type of OB is dispersive. On the contrary, the type of OB in Fig. 3(a) is absorptive as mentioned above. Comparing Fig. 6(a) with Fig. 3(a), one can conclude that the width of the hysteresis loop of dispersive OB is narrower than that of the absorptive one. In Fig. 6(b), the parameters are the same as those in Fig. 4(a) except for $\delta_p = 0.18$. In such case,

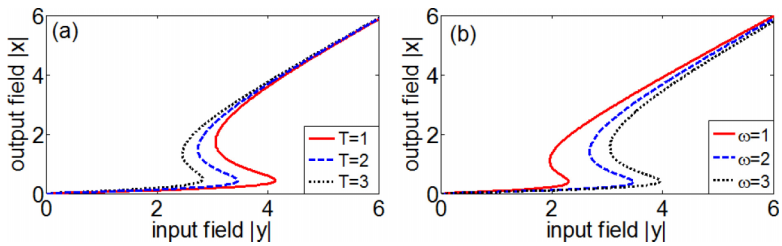

FIG. 6. (a) Output intensity $|x|$ versus input intensity $|y|$ for different value of T. Parameters are $\delta_p = 0.25$ and $\omega = 2$. (b) Output intensity $|x|$ versus input intensity $|y|$ for different value of ω. Parameters are $\delta_p = 0.18$ and $T = 2$. Other parameters are the same as those in Fig. 2.

from the solid line ($\omega = 3$) in Fig. 4(c) and 4(d), the type of OB is dispersive. Comparing with the absorptive OB in Fig. 4(a), the width of the hysteresis loop of dispersive OB is also narrower than that of the absorptive one.

Finally, it should be pointed out that recently we have studied OB in a linear TQDs using the similar method.[55] With respect to the investigation in the linear TQDs, the advantages of that of in a triangular TQDs are in the following points. First, the linear TQDs are coupled by two cascaded tunnelings, forming a four-level Λ type configuration. Thus the electrons will not tunnel to other QDs without the first tunneling, and in such case the linear TQDs will reduce to a single QD and no quantum interference exists. While in triangular TQDs, two tunnelings couple QDs individually and create a four-level tripod type configuration, therefore, the electrons can still tunnel to other QD and quantum interference exists even when one of the tunneling is missing. In addition, the method for the calculation of the triangular TQDs makes it possible to extend the study in a multiple QDs system.[45] More importantly, the previous study is lack of stating how the third-order dispersion influences the OB properties. But in the present paper, through finding the same value of third-order absorption under various tunneling parameters [the cross point in Fig. 3(c) and 4(c)], the impact of third-order dispersion on OB properties is found, that is, the larger value of nonlinear dispersion will lead to the smaller threshold of OB. Furthermore, the impact of the types of OB on hysteresis loop is also found. And these two new findings make the theoretical investigation on OB in TQDs more completed. Overall, it is hoped that this paper will stimulate experimental progress in triangular TQDs.

IV. CONCLUSIONS

In the present paper, we investigate the OB behavior as well as the third-order nonlinearity in triangular TQDs coupled by two tunnelings. The two tunnelings induce the quantum interference and modify both the linearity and the nonlinearity of the system. As a consequence, the type, the threshold and the hysteresis loop of OB can be controlled by the tunneling parameters and the probe laser field. The investigations give insights for future applications and experiments of optical switching process.

ACKNOWLEDGMENTS

This work is supported by the financial support from the National Natural Science Foundation of China (Grant Nos. 11304308, 11204029, 61306086, 61176046 and 61404138), the National Basic Research Program of China (Grant Nos. 2013CB933300), the International Science Technology Cooperation Program of China (No. 2013DFR00730), and Jilin Provincial Natural Science Foundation (Grant Nos. 20140101203JC and 20140520127JH).

APPENDIX

The analytical expressions of ρ_{10} can be obtained by solving Eq. (4). Under the steady-state condition, Eq. (4b)-(4d) can be set to zero,

$$-\Omega_p a_0 - T_2 a_2 - T_3 a_3 + \Gamma_1 a_1 = 0, \tag{A1a}$$

$$-T_2 a_1 + \Gamma_2 a_2 = 0, \tag{A1b}$$

$$-T_3 a_1 + \Gamma_3 a_3 = 0, \tag{A1c}$$

where $\Gamma_1 = \delta_p - i\gamma_1$, $\Gamma_2 = \delta_p - \omega_{12} - i\gamma_2$, $\Gamma_3 = \delta_p - \omega_{13} - i\gamma_3$.

From Eq. (A1b),

$$a_2 = \frac{T_2 a_1}{\Gamma_2} \tag{A2a}$$

From Eq. (A1c),

$$a_3 = \frac{T_3 a_1}{\Gamma_3} \tag{A2b}$$

Substituting Eq. (A2a) and (A2b) into Eq. (A1a), then

$$a_1 = \frac{\Omega_p}{\Gamma_1 - \frac{T_2^2}{\Gamma_2} - \frac{T_3^2}{\Gamma_3}} a_0. \tag{A3}$$

Substituting Eq. (A3) into Eq. (A2a) and (A2b), then

$$a_2 = \frac{T_2}{\Gamma_2} \frac{\Omega_p}{\Gamma_1 - \frac{T_2^2}{\Gamma_2} - \frac{T_3^2}{\Gamma_3}} a_0, \tag{A4a}$$

$$a_3 = \frac{T_3}{\Gamma_3} \frac{\Omega_p}{\Gamma_1 - \frac{T_2^2}{\Gamma_2} - \frac{T_3^2}{\Gamma_3}} a_0. \tag{A4b}$$

Substituting Eq.(A3) and Eq. (A4) into $|a_0|^2 + |a_1|^2 + |a_2|^2 + |a_3|^2 = 1$, then

$$|a_0|^2 = \frac{1}{1 + \frac{{\Omega_p}^2}{\left|\Gamma_1 - \frac{T_2^2}{\Gamma_2} - \frac{T_3^2}{\Gamma_3}\right|^2} \left(1 + \frac{T_2^2}{|\Gamma_2|^2} + \frac{T_3^2}{|\Gamma_3|^2}\right)}, \tag{A5}$$

The coherence element between state $|0\rangle$ and $|1\rangle$ is

$$\rho_{10} = a_0 {a_1}^* = \frac{\Omega_p}{\Gamma_1 - \frac{T_2^2}{\Gamma_2} - \frac{T_3^2}{\Gamma_3}} |a_0|^2. \tag{A6}$$

Substituting Eq. (A5) into Eq. (A6), then

$$\rho_{10} = \frac{\Omega_p}{\Gamma_1 - \frac{T_2^2}{\Gamma_2} - \frac{T_3^2}{\Gamma_3}} \frac{1}{1 + \frac{{\Omega_p}^2}{\left|\Gamma_1 - \frac{T_2^2}{\Gamma_2} - \frac{T_3^2}{\Gamma_3}\right|^2} \left(1 + \frac{T_2^2}{|\Gamma_2|^2} + \frac{T_3^2}{|\Gamma_3|^2}\right)}, \tag{A7}$$

[1] H. M. Gibbs, S. L. McCall, and T. N. C. Venkatesan, Phys. Rev. Lett. **36**, 1135 (1976).
[2] E. Abraham and S. D. Smith, Rep. Prog. Phys. **45**, 815 (1982).
[3] A. T. Rosenberger, L. A. Orozco, and H. J. Kimble, Phys. Rev. A **28**, 2569 (1983).
[4] L. A. Orozco, H. J. Kimble, A. T. Rosenberger, L. A. Lugiato, M. L. Asquini, M. Brambilla, and L. M. Narducci, Phys. Rev. A **39**, 1235 (1989).
[5] G. Rempe, R. J. Thompson, R. J. Brecha, W. D. Lee, and H. J. Kimble, Phys. Rev. Lett. **67**, 1727 (1991).
[6] A. Lambrecht, E. Giacobino, and J. M. Courty, Opt. Commun. **115**, 199 (1995).
[7] T. Ackemann, A. Heuer, Y. A. Logvin, and W. Lange, Phys. Rev. A **56**, 2321 (1997).
[8] D. F. Walls and P. Zoller, Opt. Commun. **34**, 260 (1980).
[9] W. Harshawardhan and G. S. Agarwal, Phys. Rev. A **53**, 1812 (1996).
[10] H. Wang, D. J. Goorskey, and M. Xiao, Phys. Rev. A **65**, 011801 (2001).
[11] A. Joshi, A. Brown, H. Wang, and M. Xiao, Phys. Rev. A **67**, 041801 (2003).
[12] A. Joshi and M. Xiao, Phys. Rev. Lett. **91**, 143904 (2003).
[13] A. Joshi, W. Yang, and M. Xiao, Phys. Rev. A **68**, 015806 (2003).
[14] J. Sheng, U. Khadka, and M. Xiao, Phys. Rev. Lett. **109**, 223906 (2012).
[15] H. Chang, H. Wu, C. Xie, and H. Wang, Phys. Rev. Lett. **93**, 213901 (2004).
[16] M. A. Antón, O. G. Calderón, S. Melle, I. Gonzalo, and F. Carreño, Opt. Commun. **268**, 146 (2006).
[17] J. H. Li, X. Y. Lü, J. M. Luo, and Q. J. Huang, Phys. Rev. A **74**, 035801 (2006).
[18] J. Yuan, W. Feng, P. Li, X. Zhang, Y. Zhang, H. Zheng, and Y. Zhang, Phys. Rev. A **86**, 063820 (2012).
[19] L. Wang, A. Rastelli, S. Kiravittaya, M. Benyoucef, and O. G. Schmidt, Adv. Mater. **21**, 2601 (2009).
[20] J. M. Villas-Bôas, A. O. Govorov, and S. E. Ulloa, Phys. Rev. B **69**, 125342 (2004).
[21] H. S. Borges, L. Sanz, J. M. Villas-Bôas, and A. M. Alcalde, Phys. Rev. B **81**, 075322 (2010).
[22] N. Sköld, A. Boyer de la Giroday, A. J. Bennett, I. Farrer, D. A. Ritchie, and A. J. Shields, Phys. Rev. Lett. **110**, 016804 (2013).
[23] A. Boyer de la Giroday, N. Sköld, R. M. Stevenson, I. Farrer, D. A. Ritchie, and A. J. Shields, Phys. Rev. Lett. **106**, 216802 (2011).
[24] K. Müller, A. Bechtold, C. Ruppert, M. Zecherle, G. Reithmaier, M. Bichler, H. J. Krenner, G. Abstreiter, A. W. Holleitner, J. M. Villas-Boas, M. Betz, and J. J. Finley, Phys. Rev. Lett. **108**, 197402 (2012).
[25] K. M. Weiss, J. M. Elzerman, Y. L. Delley, J. Miguel-Sanchez, and A. Imamoğlu, Phys. Rev. Lett. **109**, 107401 (2012).
[26] C. H. Yuan and K. D. Zhu, Appl. Phys. Lett. **89**, 052115 (2006).
[27] H. S. Borges, L. Sanz, J. M. Villas-Boas, and A. M. Alcalde, Appl. Phys. Lett. **103**, 222101 (2013).
[28] E. Paspalakis, A. Kalini, and A. F. Terzis, Phys. Rev. B **73**, 073305 (2006).
[29] H. F. Yao, N. Cui, Y. P. Niu, and S. Q. Gong, Photon. Nanostructures **9**, 174 (2011).

[30] A. Fountoulakis and E. Paspalakis, J. Appl. Phys. **113**, 174301 (2013).
[31] E. Voutsinas, A. F. Terzis, and E. Paspalakis, Phy. Lett. A **378**, 219 (2014).
[32] J. Li, R. Yu, J. Liu, P. Huang, and X. Yang, Physica E **41**, 70 (2008).
[33] Z. Wang, S. Zhen, X. Wu, J. Zhu, Z. Cao, and B. Yu, Opt. Commun. **304**, 7 (2013).
[34] H. Jafarzadeh, M. Sahrai, and K. Jamshidi-Ghaleh, Eur. Phys. J. D **68**, 115 (2014).
[35] Z.P. Wang and B.L. Yu, J. Opt. Soc. Am. B **30**, 2915 (2014).
[36] M. T. Cheng, X. S. Ma, Y. Q. Luo, P. Z. Wang, and G. X. Zhao, Appl. Phys. Lett. **99**, 223509 (2011).
[37] S. Liu, R. Yu, J. Li, and Y. Wu, J. Appl. Phys. **115**, 134312 (2014).
[38] S. C. Tian, C. Z. Tong, C. L. Wang, L. J. Wang, H. Wu, E. B. Xing, Y. Q. Ning, and L. J. Wang, Opt. Commun. **312**, 296 (2014).
[39] Y. D. Peng, A. H. Yang, D. H. Li, H. Zhang, Y. P. Niu, and S. Q. Gong, Laser Phys. Lett. **11**, 065201 (2014).
[40] Q. Xie, A. Madhukar, P. Chen, and N. P. Kobayashi, Phys. Rev. Lett. **75**, 2542 (1995).
[41] R. Songmuang, S. Kiravittaya, and O. G. Schmidt, Appl. Phys. Lett. **82**, 2892 (2003).
[42] G. Rainò, A. Salhi, V. Tasco, M. De Vittorio, A. Passaseo, R. Cingolani, M. De Giorgi, E. Luna, and A. Trampert, J. Appl. Phys. **103**, 096107 (2008).
[43] C. Y. Hsieh, Y. P. Shim, M. Korkusinski, and P. Hawrylak, Rep. Prog. Phys. **75**, 114501 (2012).
[44] R. Yu, J. Li, C. Ding, and X. Yang, Phy. Lett. A **375**, 2738 (2011).
[45] S. C. Tian, C. Z. Tong, R. G. Wan, Y. Q. Ning, and L. J. Wang, arXiv:1310.4599 2013.
[46] S. C. Tian, R. G. Wan, E. B. Xing, C. Z. Tong, and Y. Q. Ning, J. Mod. Opt. **61**, 1479 (2014).
[47] S. C. Tian, R. G. Wan, C. Z. Tong, Y. Q. Ning, L. Qin, and Y. Liu, J. Opt. Soc. Am. B **31**, 1436 (2014).
[48] S. C. Tian, C. Z. Tong, and C. L. Wang, Y. Q. J. Lumin. **153**, 169 (2014).
[49] M. R. Mehmannavaz, R. Nasehi, H. Sattari, and M. Mahmoudi, Superlattices and Microstructures **75**, 27 (2014).
[50] H. Reza Hamedi, Physica B **449**, 5 (2014).
[51] G. S. Agarwal, *Quantum Optics* (Springer-Verlag, Berlin, 1974).
[52] S. M. Barnett and P. M. Radmore, *Methods in Theoretical Quantum Optics* (Oxford University Press, Oxford, 1997).
[53] R. Bonifacio and L. A. Lugiato, Phys. Rev. A **18**, 1129 (1978).
[54] P. Meystre, Opt. Commun. **26**, 277 (1978).
[55] S. C. Tian, R. G. Wan, C. Z. Tong, and Y. Q. Ning, J. Opt. Soc. Am. B **31**, 2681 (2014).